Analysis of a Liquid Crystal Fabry–Perot Etalon Filter: A Novel Model

Po-Lun Chen, Kuen-Cherng Lin, Wei-Ching Chuang, Yen-Chang Tzeng, Kun-Yi Lee, and Wei-Yu Lee

***Abstract*— The authors propose a novel analysis method to investigate the characteristics of an electrically tunable liquid-crystal Fabry–Perot interferometer (LC-FPI). Based on the solution of deformation analysis of liquid crystal in an electric field and the assumption of small refractive index variation in the Fabry–Perot cavity, the voltage-dependent equivalent refractive index of the cavity has been derived. Tuning behaviors of the LC-FPI filter were simulated by means of the dependence. The calculated result and the experimental measured data agree well with each other.**

***Index Terms*—Fabry–Perot interferometer, filter, liquid crystal.**

I. Introduction

IN RECENT YEARS, there has been a growing interest in tunable wavelength-selective filters using liquid crystal [1]–[4] for high-density wavelength division multiplexing (HD-WDM) systems. The promising properties of electrically tunable liquid crystal Fabry–Perot interferometers (LC-FPI), such as simple structure, low loss, low drive, narrow bandwidth, and wide tunable range, have led to their rapid applications [5]–[8] as crucial components in optical fiber communication. The filter can be widely tuned with an application of 1–5 V that changes the optical path length in the cavity of a Fabry–Perot etalon.

However, there is still no powerful simulation model as a design tool for the LC-FPI's. In this letter, we propose a simple analysis method to explore the voltage-dependent transmission and filter bandwidth characteristics of electrically tunable liquid crystal Fabry–Perot interferometers. The model is based on deformation analysis of liquid crystal in an electric field and derivation of the equivalent refractive index of the liquid crystal. Via the combination of both, the voltage-dependent refractive index function, which is the fundamental of the proposed model, was given and the filter characteristics of the LC-FPI were simulated.

II. Model Concept

The basic structure of an electrically tunable LC-FPI is shown in Fig. 1. A homogeneously aligned nematic LC layer is sandwiched between two glass plates, on which alignment films, indium tin oxide (ITO) transparent electrodes, and dielectric mirrors were deposited. An electric field is applied to the LC via ITO electrodes deposited upon the inner sides of the glass plates. The outer sides are coated with an antireflective film. Nematic liquid crystal exhibits high-birefringent and electrooptic effects because of the field-induced orientation of the molecules.

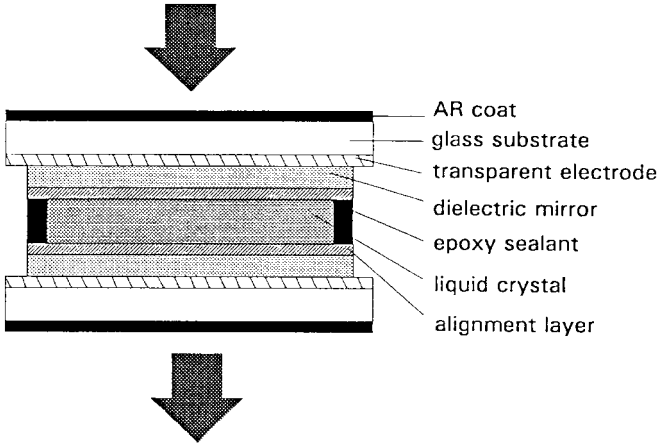

Fig. 1. The basic structure of a tunable LC-FPI.

The substrate surfaces are assumed to be rubbing-treated along the surface plane of the glass plates; thus, the LC molecules are aligned along the same direction, say, in an x direction. When an external electric field is applied, the LC molecules tilt at an angle ϕ relative to the x axis to increase the elastic energy but lower the electrostatic energy. Thus, the light linearly polarized along the x direction experiences the refractive index [9]

$$n(\phi) = \frac{n_e \cdot n_0}{\sqrt{n_e^2 \sin^2\phi + n_o^2 \cos^2\phi}} \tag{1}$$

depending on the tilted angle ϕ, where n_o and n_e are the ordinary and extraordinary refractive indices of the LC, respectively. On the other hand, the position-dependent tilted angle $\phi(z)$ can be derived by the deformation of nematic LC's in an electric field, which has been solved by Deuling [10],

$$\frac{2z}{L} \cdot \int_0^{\phi(L/2)} \left(\frac{(1+\kappa\sin^2\phi)(1+\gamma\sin^2\phi)}{\sin^2\phi(L/2) - \sin^2\phi} \right)^{1/2} d\phi = \int_0^{\phi} \left(\frac{(1+\kappa\sin^2\phi)(1+\gamma\sin^2\phi)}{\sin^2\phi(L/2) - \sin^2\phi} \right)^{1/2} d\phi \tag{2}$$

where L is thickness of the LC cells, $\kappa = \kappa_{33}/\kappa_{11} - 1$ and $\gamma = \varepsilon_{//}/\varepsilon_{\perp} - 1$. κ_{33} and κ_{11} are the elastic constants for splay

Manuscript received September 16, 1996; revised December 19, 1996. This work was supported by the National Science Council of the Republic of China under Contract NSC85-2612-E150-002 and Contract NSC86-2215-E036-001.

P.-L. Chen is with the Institute of Electro-optic, National Chiao-Tung University, Hsin-Chu, Taiwan R.O.C.

K.-C. Lin, K.-Y. Lee, and W.-Y. Lee are with the Department of Electrical Engineering, Tatung Institute of Technology, Taipei, Taiwan, R.O.C.

W.-C. Chuang is with the Department of Electro-Optic, National Yunlin Polytech Institution, Yunlin, Taiwan R.O.C.

Y.-C. Tzeng is with the Institute of Nuclear Energy Research, Lung-Tan, Taiwan R.O.C.

Publisher Item Identifier S 1041-1135(97)02443-9.

TABLE I
THE MODEL PARAMETERS USED IN THE ANALYSIS

Ordinary refractive index of the NLC	$n_o = 1.4771$
Extraordinary refractive index of the NLC	$n_e = 1.5506$
Elastic constant ratio of the NLC	$\kappa_{33}/\kappa_{11} = 1.28$
Relative parallel dielectric constants of the NLC	$\varepsilon_{//} = 5.9$
Relative perpendicular dielectric constants of the NLC	$\varepsilon_{\perp} = 3.5$
Size of spacer	$d = 10\ \mu m$

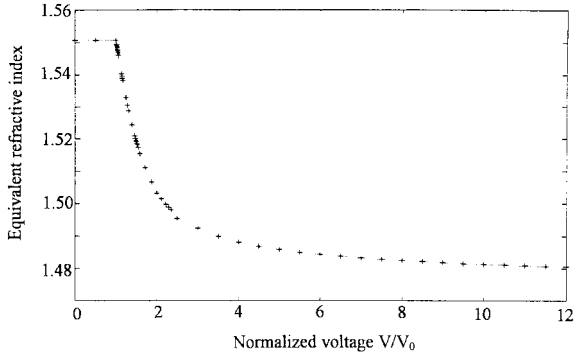

Fig. 2. Equivalent refractive index as a function of the normalized voltage V/V_0.

and bend, respectively. $\varepsilon_{//}$ and $\varepsilon_{\perp}$ are the relative dielectric constants parallel and perpendicular to the direction of the molecules, respectively. From the above two equations, the refractive index profile $n(z)$ across the cavity can be obtained.

Assuming the refractive-index differences between any two adjacent layers in an ν-layer Fabry–Perot cavity are small, the total resonance order can be summarized as

$$m_{\text{total}} = \sum_{i=1}^{\nu} m_i \tag{3}$$

where m_i is resonance order in the ith layer. Since $m_i = 2n_i d_i/\lambda_i$, the above equation can be derived as

$$n_{\text{equ}} = \frac{1}{d}\sum_{i=1}^{\nu} n_i d_i \tag{4}$$

where d is the cavity length. Thus, the equivalent refractive index of the whole cavity can be defined as

$$n_{\text{equ}} = \frac{1}{d}\int_0^d n(z)\,dz. \tag{5}$$

To explore the effect of the external electric field, $\phi(L/2)$ in (2) was obtained for any given value of the applied voltage V by [10]

$$\frac{2}{\pi}\sqrt{1+\gamma\sin^2\phi(L/2)} \cdot \int_0^{\phi(L/2)} \left(\frac{(1+\kappa\sin^2\phi}{(1+\gamma\sin^2\phi)(\sin^2\phi(L/2)-\sin^2\phi)}\right)^{1/2} d\phi = \frac{V}{V_0} \tag{6}$$

where

$$V_0 = \pi\sqrt{\frac{\kappa_{11}}{\varepsilon_0(\varepsilon_{//}-\varepsilon_{\perp})}}$$

refers to the threshold voltage of the LC. Thus, by combining (1), (2), (5), and (6), we can obtain the equivalent refractive index as a function of the applied voltage, which facilitates the analysis of LC-FPI filters.

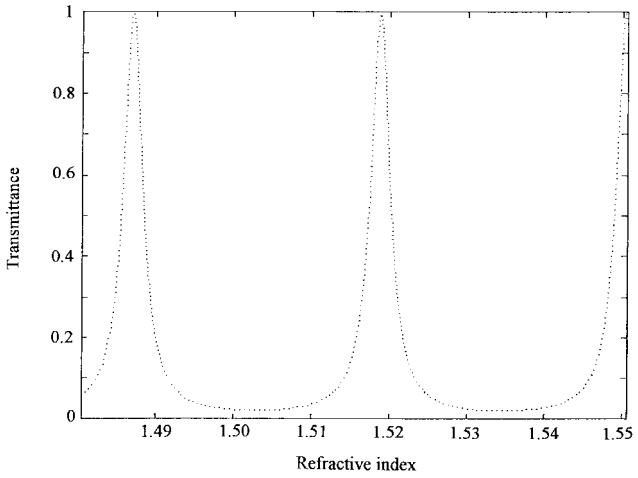

Fig. 3. The refractive index dependency of the filter transmission, where unity transmission peaks indicate the values of n_{equ} under resonance conditions.

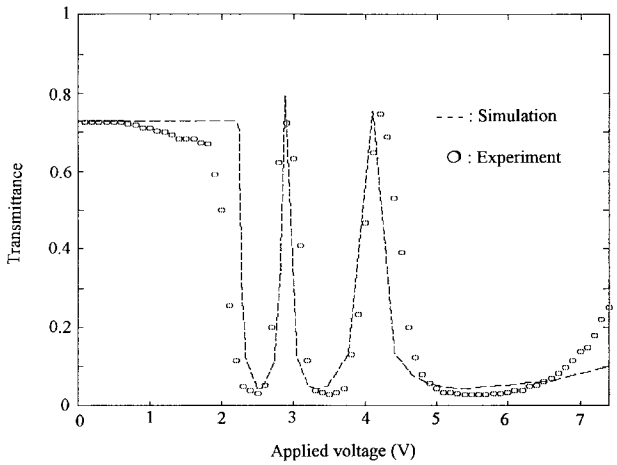

Fig. 4. The electrically tuning transmission characteristics as a function of applied voltage, where the circle signs indicate the measured data of the filter with the same structure parameters. The reflectivity R of the dielectric mirrors was assumed to be 0.7 in the simulation.

III. RESULTS AND DISCUSSION

In order to show the applicability of the concept of the proposed model, we considered an LC-FPI filter of the nematic LC (Merck ZLI-3103) with its structural parameters shown in Table I. The application of nematic liquid crystals to construct an electrically tunable FPI filter is feasible due to the deformation effect of the LC. The He–Ne laser source with a wavelength 633 nm was utilized due to its visibility to facilitate the characteristic measurement and the finding of a prototype result. By using the model described in the last section, we calculated the equivalent refractive index as a function of the normalized voltage V/V_0. The result is plotted in Fig. 2. If the applied voltage is lower than the threshold voltage ($V_0 = 2.2$ V), n_{equ} would equal n_e; otherwise, n_{equ} would be tunable and decrease from n_e to n_o monotonously. The voltage-dependent equivalent refractive index function is an important base to explore the characteristics of the filters.

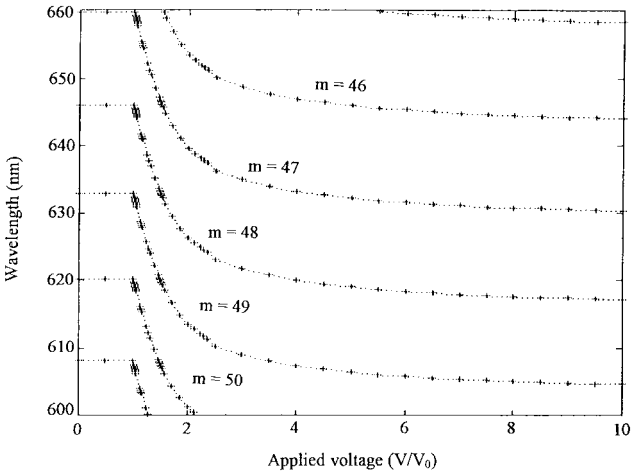

Fig. 5. The center wavelength of the filter passband versus applied voltage. m denotes the resonance order.

Moreover, this threshold effect is crucial in practical design of the electrically tunable LC-FPI filter.

Since the optical path length of a Fabry–Perot etalon is strongly affected by the overall refractive index profile of the cavity, the transmission can be inferred to be $n_{\rm equ}$-dependent. Fig. 3 shows the refractive index dependency of the transmission, where unity transmission peaks indicate the values of $n_{\rm equ}$ under resonance conditions. This plot can be easily obtained via the operational principle of a Fabry–Perot etalon. The sharpness of the transmission peaks can be increased using either a larger cavity or a pair of higher-reflectivity mirrors; however, the former would induce a small free spectra range (FSR) and the latter would decrease the overall transmitted intensity.

Combining Figs. 2 and 3, the voltage-dependent transmission characteristics were obtained and shown in Fig. 4, where the circle signs indicate the measured data of the filter with structure parameters shown in Table I. The parameters of the nematic LC were given by the supplier, while the LC cell thickness was extracted by fitting the measurement. Resonance condition of the LC-FPI filter shifts as the refractive index of the liquid crystal changes, or equivalently, as the applied voltage changes. Note that the full voltage-width of the half maximum in voltage-dependent transmission characteristics corresponds to the full bandwidth of the half maximum in wavelength-dependent transmission characteristics. Thus, the FWHM (full width at half maximum) can be estimated with the help of this figure. As can be seen, the experimentally measured data agree considerably with the calculated one. The little discrepancy can be due to the fact that the LC molecules close to the alignment surface do not reorient even though the applied voltage is sufficient. This result supports the validity of the proposed model.

Fig. 5 shows the tuning characteristics of the passband center wavelength as a function of the applied voltage. From this figure, the FSR of the LC-FPI filter can be found. Besides, we can see the threshold effect of the filter, i.e., the wavelength tuning begins in case the applied voltage exceeds the threshold value of 2.2 V. Almost all performance characteristics of a tunable LC-FPI filter could be simulated by using the voltage-dependent equivalent refractive index characteristics.

IV. Conclusion

To investigate electrically tunable liquid-crystal Fabry–Perot interferometers, we proposed a simple method to analyze their characteristics. Based on the solution of deformation analysis of liquid crystal in an electric field and the assumption of small refractive index variation in the Fabry–Perot cavity, the voltage-dependent equivalent refractive index of the cavity has been derived. By means of the dependence, tuning behaviors of the LC-FPI filter were simulated. Good agreement between theoretical calculation and experimental measured data implies the validity of our method.

Acknowledgment

The authors would like to appreciate Dr. H. H. Lin for his valuable editorial assistance.

References

[1] S. Mallinson, "Wavelength-selective filters for single-mode fiber WDM systems using Fabry–Perot interferometer," *Appl. Opt.,* vol. 26, pp. 430–436, 1987.

[2] M. W. Maeda, J. S. Patel, and L. Chinlon, J. Horrobin, and R. Spicer, "Electrically tunable liquid-crystal etalon filter for high-density WDM system," *IEEE Photon. Technol. Lett.*, vol. 2, pp. 820–822, 1990.

[3] J. S. Patel, M. A. Saifi, D. W. Berreman, L. Chinlon, N. Andreadakis, and S. D. Lee, "Electrically tunable optical filter for infrared wavelength using liquid crystal in a Fabry–Perot etalon," *Appl. Phys. Lett.,* vol. 57, pp. 1718–1719, 1990.

[4] K. Hirabayashi, H. Tsuda, and T. Kurokawa, "Narrow-band tunable wavelength-selective filters of Fabry-Perot interferometer with liquid-crystal intracavity," *IEEE Photon. Technol. Lett.,* vol. 3, pp. 213–215, 1991.

[5] Y. Suzuki, N. Ohta, and K. Hirabayashi, "Nonlinear distortion due to Fabry–Perot optical filter in direct modulated dense WDM-SCM video distribution systems," *IEEE Photonic Technol. Lett.,* vol. 4, pp. 466–468, 1993.

[6] H. Tsuda, K. Firabayashi, Y. Tohmori, and T. Kurokawa, "Tunable light source using a liquid-crystal Fabry–Perot interferometer," *IEEE Photon. Technol. Lett.,* vol. 3, pp. 504–506, 1991.

[7] H. Tsuda, H. Uenohara, H. Iwamura, K. Hirabayashi, and T. Kurokawa, "Tunable wavelength conversion using a liquid crystal filter and a bistable laser diode," *Appl. Phys. Lett.*, vol. 61, pp. 2006–2008, 1992.

[8] K. Hirabayashi and T. Kurokawa, "Tunable wavelength-selective demultiplexer using a liquid crystal filter," *IEEE Photon. Technol. Lett.,* vol. 4, pp. 737–740, 1992.

[9] A. Yariv and P. Yeh, *Optical Waves in Crystals.* New York: Wiley, 1984, pp. 266–270.

[10] H. J. Deuling, "Deformation of nematic liquid crystals in an electric field," *Mol. Cryst. and Liquid Cryst.,* vol. 19, pp. 123, 1972.